

# TIMP-3, Collagen, and Elastin Immunohistochemistry and Histopathology of Sorsby's Fundus Dystrophy

N. H. Victor Chong,<sup>1,2</sup> Robert A. Alexander,<sup>1</sup> Trevor Gin,<sup>2</sup> Alan C. Bird,<sup>2</sup> and Philip J. Luthert<sup>1</sup>

**PURPOSE.** Mutations in the tissue inhibitor of metalloproteinases-3 (*TIMP-3*) gene have previously been identified in patients with Sorsby's fundus dystrophy (SFD). We evaluated the ocular distribution of TIMP-3 and other extracellular constituents in SFD.

**METHODS.** The eyes of an SFD donor with a confirmed TIMP-3 mutation were examined using histologic techniques demonstrating connective tissue, calcium, and lipid. Immunohistochemical analyses were performed using antibodies against TIMP-3, collagen type IV, V, and VI, laminin, fibronectin, elastin, and fibrillin. Electron microscopy also was used.

**RESULTS.** A subretinal pigment epithelium (sub-RPE) deposit similar to that previously described was seen. A morphologically similar but different deposit was present internal to the nonpigmented ciliary epithelium (NPCE). Both deposits contained collagens, elastin, glycosaminoglycans, lipids, and calcium. Immunolabeling of TIMP-3 was found in the basement membrane of the NPCE, Bruch's membrane, and choroidal vessels in normal control subjects. In SFD, immunolabeling of TIMP-3 also was present in the sub-RPE deposit and in the inner portion of the ciliary body deposit. TIMP-3 immunoreactivity was more extensive in the SFD eye. The pattern of elastin immunoreactivity was remarkably similar to that of TIMP-3. Electron microscopy revealed a morphologically altered elastic layer of the Bruch's membrane.

**CONCLUSIONS.** Sub-RPE TIMP-3 immunoreactivity appears more extensive in SFD than in control subjects. There is also a correspondence between TIMP-3 and elastin immunoreactivities, which invites speculation as to a link between the SFD TIMP-3 mutation and altered elastin processing. The accumulation of abnormal material in SFD is more widespread than previously reported. In view of this, SFD might be better termed Sorsby's ocular epitheliopathy. (*Invest Ophthalmol Vis Sci.* 2000;41:898-902)

In 1949 Sorsby and colleagues described four families with late-onset, autosomal dominant inheritance of macular dystrophy.<sup>1</sup> The fundal features are similar to those of exudative age-related macular degeneration (AMD) but are present at a younger age.<sup>2-4</sup> In the third or fourth decade patients have poor night vision, followed by the loss of central vision, usually secondary to geographic atrophy or choroidal neovascularization (CNV) in the fifth decade. It has become clear that not only the macula but the whole retina is affected, because progressive loss of peripheral vision is also common.<sup>4</sup> Weber and colleagues demonstrated linkage of the condition to chromosome 22q13ter<sup>5</sup> and subsequently identified a point mutation in the tissue inhibitor of metalloproteinases-3 (*TIMP-3*) gene.<sup>6</sup> *TIMP-3* is known to be a component of Bruch's membrane<sup>7</sup> and is expressed by retinal pigment epithelial (RPE) cells.<sup>8</sup>

There are two previous histologic reports of the condition. Ashton and Sorsby<sup>9</sup> reported two sisters with clinical features similar to SFD. There was, however, no family history and they were not among the original family pedigrees. It has been suggested that these two sisters might have had either a complication of AMD or dominant drusen rather than SFD. Capon and colleagues<sup>10</sup> reported the light and electron microscopy findings of a descendant of one of the original pedigrees of SFD. They described a layer of lipid-positive floccular deposit that was up to 30  $\mu\text{m}$  in thickness, on the inner aspect of Bruch's membrane. The composition of this deposit remains unknown. The anterior segments of these eyes were not described.

In this article, we report the histologic and immunohistochemical findings in both the anterior and posterior segments of the eye of an SFD patient with a confirmed *TIMP-3* mutation. The localization of TIMP-3 in both normal and SFD eyes also was examined.

## MATERIALS AND METHODS

### Clinical History

The eyes of a 77-year-old white woman with SFD caused by the Ser-181-Cys *TIMP-3* mutation were obtained postmortem. She was patient IV-4 in Pedigree Plate IV of the original report by Sorsby and colleagues.<sup>1</sup> At that time, she was 29-years-old and

---

From the Departments of <sup>1</sup>Pathology and <sup>2</sup>Clinical Ophthalmology, Institute of Ophthalmology, University College London; and Moorfields Eye Hospital, London, England.

Supported by an LORS grant from Moorfields Eye Hospital, London. NHVC is an MRC Clinical Training Fellow.

Submitted for publication February 17, 1998; revised August 20, 1998, November 12, 1998, June 10, 1999, and September 28, 1999; accepted September 29, 1999.

Commercial relationships policy: N.

Corresponding author: Victor Chong, Professorial Unit, Moorfields Eye Hospital, City Road, London, EC1V 2PD, England. v.chong@ucl.ac.uk

was reported to be normal. She became symptomatic in her early thirties, with deteriorating night vision. In her early forties, she presented with distorted vision in her left eye, followed by central visual loss secondary to CNV. One year later, this was followed by visual loss in her right eye. Visual acuities were hand motion at 1 m, and she was found to have bilateral disciform macular scars. At the age of 57 years, she had a left-sided, total retinal detachment, which was repaired successfully with an encircling band. She had right-sided cataract surgery with an intraocular implant in her 70s.

### Fixation and Processing

The right eye was fixed in 0.25% glutaraldehyde and 4% paraformaldehyde in phosphate-buffered saline, and the left eye was fixed in 10% formol saline for 48 hours. Specimens for light microscopy and immunohistochemistry were processed through ascending concentrations of alcohol into xylene and infiltrated with paraffin wax. Five-micron-thick sections were dewaxed and rehydrated before use. Specimens for lipid analyses were frozen in liquid nitrogen-cooled isopentane. Ten-micron-thick cryostat sections were cut. Specimens for electron microscopy were postfixated in osmium tetroxide, processed through ascending concentrations of ethanol, and finally infiltrated with Araldite resin.

### Staining Techniques

Hematoxylin and eosin was used for general morphology. Mowry and Marand Alcian blue/periodic acid-Schiff (PAS), Gomori aldehyde fuchsin, Fullmer and Lillie oxidation aldehyde fuchsin, and Verhoeff techniques were used for demonstrating different classes of glycosaminoglycans and elastic fibers at different stages of maturity. McGee-Russel alizarin red S technique and the Pizzolato silver method were used to demonstrate calcium. Congo red staining was used to exclude amyloid. Oil red O was used on frozen sections to demonstrate lipid.

The distribution of TIMP-3 (Triple Point Biologics, Forest Grove, OR), type IV collagen (Dako Ltd., High Wycombe, England), type V collagen (Chemicon Ltd, Harrow, UK), type VI collagen (Chemicon Ltd.), fibrillin (Chemicon Ltd.), fibronectin (Dako Ltd.), laminin (Dako Ltd.), and elastin (Elastin Company, MO) were investigated using a standard biotin-streptavidin biotin, alkaline phosphatase complex method (Dako Ltd.). The alkaline phosphatase label was visualized as a red final reaction product (Vector Ltd., Peterborough, England). Nuclei were weakly stained with Mayer's hematoxylin. TIMP-3, elastin, and fibronectin antibodies had been raised in rabbit, and the others were mouse monoclonals.

Antigen retrieval was utilized in all cases. Sections for TIMP-3 and fibrillin required pressure cooking. Sections for fibronectin, laminin, and elastin demonstration were exposed to 0.1% trypsin for 15 minutes at 37°C, whereas types IV, V, and VI collagen sections received 0.4% pepsin treatment for 60 minutes at 37°C. Electron microscopic semithin sections were stained with toluidine blue, and ultrathin sections were stained using lead citrate and uranyl acetate.

Special stains, immunohistochemistry, and electron microscopy also were carried out in a normal donor eye from a 72-year-old normal female donor for comparison. This eye was fixed in 10% formol saline and was treated exactly as the SFD eye as described above. The son of the SFD donor, aged 57

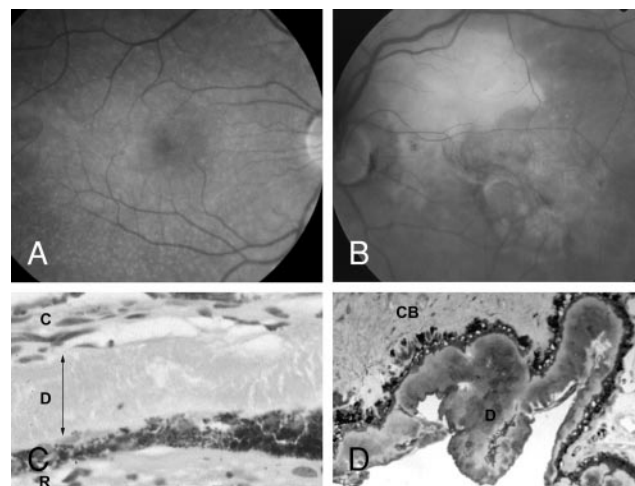


**FIGURE 1.** Clinical pictures and light microscopy of Sorsby fundus dystrophy. (A) Right fundal picture of the son of the donor aged 57 years, with the same condition showing multiple drusen; (B) left fundal picture of the son of the donor aged 57 years with the same condition showing a disciform scar secondary to previous choroidal neovascularization. (C) H&E  $\times 660$ , showing the subretinal deposits (arrows indicate the extent); (D) toluidine blue  $\times 400$ , showing ciliary body deposit. C, choroid; CB, ciliary body; D, deposit; R, neurosensory retina.

years, also was affected; his right fundal picture showed widespread, drusenlike structures at the posterior pole (Fig. 1A), whereas his left fundal picture showed a disciform macular scar (Fig. 1B).

## RESULTS

### Gross Examination

The right eye was of normal size and was opened vertically. Intraocular examination revealed a one-piece poly(methyl methacrylate) (PMMA) intraocular implant within the lens capsule. The vitreous was attached and there was irregular discoloration of the retina with dark, pale, and yellowish patches. The left eye was distorted, and an encircling band was present. Intraocular examination revealed widespread pigmentary abnormalities of the attached posterior pole of the retina, with areas of pallor and dusky, yellowish pigmentation.

### Light Microscopy

The appearances of the ciliary body and posterior pole were similar in both eyes. A single-cell, thick, patchy epiretinal membrane was present. There was retinal gliosis with marked thinning of the inner nuclear layer and near total loss of photoreceptor cells. There was patchy loss and disorganization of the RPE. In many situations, an up to 30  $\mu\text{m}$  thick sub-RPE layer of eosinophilic material was seen. This extended to just posterior to the ora serrata and was granular in appearance (Fig. 1C). In places, striations oriented perpendicular to Bruch's membrane were seen. Foci of looser, eosinophilic material separated the deposits from Bruch's membrane, which itself was discontinuous. Clumps of punctate mineralization also lay external to the deposit.

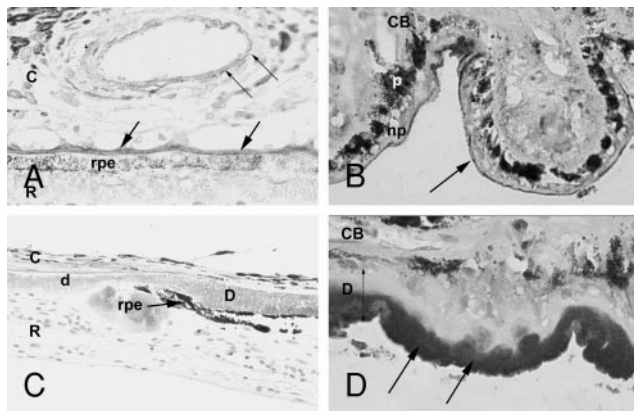


**FIGURE 2.** TIMP-3 immunohistochemistry. (A) Normal  $\times 400$ , showing labeling in Bruch membrane (*thick arrows*) and the elastic layer of choroidal vessel (*thin arrows*); (B) Normal  $\times 400$ , showing immunolabeling in the basement membrane of the nonpigmented ciliary epithelium (*arrow*); (C) Sorsby fundus dystrophy (SFD)  $\times 400$ , showing heavy immunolabeling in the deposit (D), with the presence of RPE and less immunolabeling in the deposit (d) without overlying RPE; (D) SFD (ciliary body)  $\times 400$ , showing immunolabeling only in the inner portion (*arrows*) of the ciliary body deposit (D). C, choroid; CB, ciliary body; np, nonpigmented ciliary epithelium; p, pigmented ciliary epithelium; rpe, retinal pigment epithelium; R, neurosensory retina.

In the anterior segment, a moderately uniform layer of amorphous, eosinophilic material up to  $50\ \mu\text{m}$  in thickness lay internal to the nonpigmented ciliary body epithelium (Fig. 1D). It extended onto the anterior portion of the pars plana but was not present more posteriorly. There was no deposit on the iris.

### Special Stains

The main sub-RPE deposit was PAS-positive but Alcian blue-negative. A rim of positive staining with aldehyde fuchsin was seen along portions of the outer aspect of the sub-RPE deposit, and much of the deposit was positive with oxidation aldehyde fuchsin. The elastin layer of Bruch's membrane was stained by the Verhoeff technique. It was, however, disrupted in many places. Staining with Congo red revealed no evidence of amyloid. The sub-RPE deposit was shown to contain calcium with McGee-Russel alizarin red S method but was negative with the Pizzolato silver technique for calcium oxalate. It was lipid-positive with Oil red O staining.

Restricted neovascularization was present external to or within the sub-RPE deposit. The choroid was atrophic, with total loss of the choriocapillaris in some areas, especially where the RPE was absent. Some choroidal vessels displayed diffusely thickened walls. The sclera was unremarkable, and there was atrophy of the optic nerve.

The inner portion of the deposit was positive with aldehyde fuchsin, and the outer portion of the ciliary body was positive with oxidation aldehyde fuchsin. Staining with the other special stains was quantitatively similar to that beneath the RPE. However, both the calcium and lipid staining were less intense.

### TIMP-3 Immunohistochemistry

In the normal control subject, Bruch's membrane, the elastic layer of some choroidal vessels (Fig. 2A), and the basement membrane of the nonpigmented ciliary epithelium (Fig. 2B)

were immunoreactive with TIMP-3. In the SFD eye, immunostaining for TIMP-3 was present in the entire sub-RPE deposit, and it was more intense in areas where overlying RPE cells were present (Fig. 2C). In the ciliary body deposit, however, only the inner portion was positively stained (Fig. 2D).

### Immunohistochemistry for Extracellular Matrix Components

In the control case, the elastic layer of Bruch's membrane and some of the choroidal vessels stained positively for elastin. In the SFD eye, in addition, the outer edge of the sub-RPE deposit and the inner portion of the ciliary body deposit were positively stained for elastin.

In the control and SFD eyes, an antibody to type VI collagen highlighted retinal and choroidal vessels. In the SFD eye, the outer edge of the sub-RPE deposit was immunoreactive (Fig. 3A). No positive staining was observed in the ciliary body deposit. In the control and SFD eyes, immunoreactivity for type IV collagen was present at the inner limiting membrane, the basement membrane of blood vessels, and Bruch's membrane. In addition, immunoreactivity of the inner and outer margins of the sub-RPE deposit (Fig. 3B) and a rim of ciliary body deposit just adjacent to the basement membrane was present in the SFD eye.

There were no significant differences in immunostaining for type V collagen, laminin, fibronectin, or fibrillin between control and SFD eyes.

### Electron Microscopy

The sub-RPE deposit was present between the RPE basement membrane and the elastic layer of the Bruch's membrane (Fig. 4A). It appeared to be divided into three main zones. The principle abnormality was the central electron-dense area, with a branching, frondlike appearance reminiscent of some corals. Some of this material exhibited a characteristic banding pattern typically seen in wide-spaced material (also known as long-spaced collagen) (Fig. 4B). This material was sandwiched between two layers of amorphous material containing collagen fibers.

The elastic layer of Bruch's membrane was irregular, thickened, and broken in many areas. Furthermore, the structural arrangement of the elastic component was abnormal. In the normal elastic fiber, microfibrils covered an essentially amorphous central core (Fig. 4C, top). In the SFD eye, the microfibrils

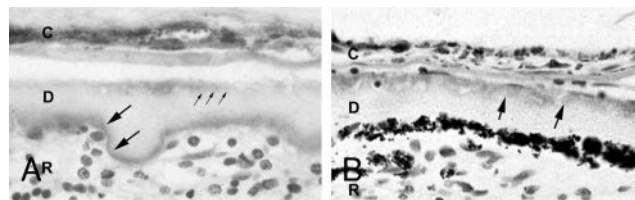


**FIGURE 3.** Collagen immunohistochemistry in Sorsby fundus dystrophy. (A) Type VI collagen in SFD  $\times 660$ , showing immunolabeling in the outer edge (*arrows*) of the deposit. (B) Type IV collagen in SFD  $\times 660$ , showing immunolabeling in the inner (*larger arrows*) and outer (*small arrows*) edges of the deposit. C, choroid; D, deposit; R, neurosensory retina.

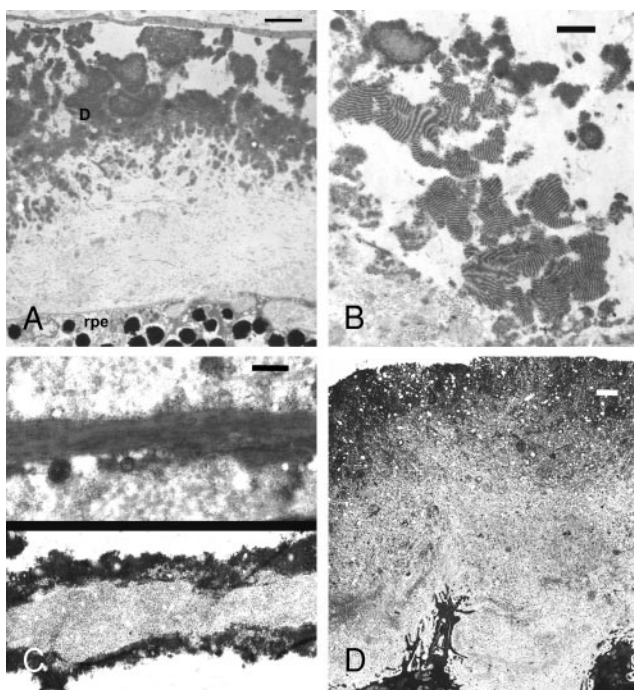


**FIGURE 4.** Electron microscopy in Sorsby fundus dystrophy (SFD). (A) SFD, showing sub-RPE deposit in the inner collagenous layer. Bar, 2  $\mu$ m. (B) SFD, showing wide-spaced material. Bar, 1  $\mu$ m. (C) Elastic layer of Bruch's membrane. *Top*: normal, showing microfibrils together with an essentially central amorphous core. *Bottom*: SFD, showing microfibrils within the central area and surrounded by amorphous material. Bar, 300 nm. (D) SFD ciliary body, showing the three layers of different electron-dense material comprising the deposit. Bar, 2  $\mu$ m.

brillar component dominated the central portion and was surrounded by amorphous material (Fig. 4C, bottom).

The outer collagenous layer of Bruch's membrane and the choroidal endothelial basement membrane were relatively normal where the elastic layer was intact. However, it was invaded by the electron-dense deposit when it was broken. Glial cell processes, cellular debris, and new vessels also were present in the deposit.

The ciliary body deposit also could be divided into three main zones (Fig. 4D). The layer adjacent to the ciliary epithelium was similar in appearance and composition to that of the loose collagen layer in the subretinal deposit. Oxytalan fibers, which correspond to the fibrous material positive with oxidation aldehyde fuchsin, were present. The middle zone consisted of a granular deposit with no definite structure. The innermost layer was more electron-dense and appeared to be composed of tightly packed material not dissimilar to that in the middle zone. Wide-spaced material, glial cell processes, cellular debris, and new vessels were not seen in any part of the ciliary body deposit.

## DISCUSSION

The sub-RPE deposit was similar in morphology to the case described by Capon and colleagues, but the anterior segment findings were not described in the previous study. After the ciliary body deposit was seen in the present case, we reviewed

sections from the study by Capon and colleagues<sup>10</sup>; the same ciliary body deposit was present.

Similar sub-RPE deposits have been observed in dominant, late-onset retinal degeneration,<sup>11</sup> dominant drusen,<sup>11</sup> dominant retinitis pigmentosa (RP),<sup>13</sup> and hypobetalipoproteinemia with RP.<sup>13</sup> In all these cases, the exact morphology and composition might be slightly different, but they all contain extracellular matrix material (including collagen, elastin, and glycoaminoglycans) with or without calcium and lipids.<sup>11-13</sup> It is possible that the accumulation of these extracellular materials might be a nonspecific response to changes in Bruch's membrane.

## TIMP-3 Mutation and the Deposits

TIMP-3 is an inhibitor of matrix metalloproteinases (MMPs), and MMPs break down connective tissue material in the extracellular matrix. It is, therefore, perhaps unexpected to find a mutation in *TIMP-3* associated with an increased accumulation of extracellular material, unless the mutant TIMP-3 shows gain of function. There is, however, evidence to suggest that mutant TIMP-3 forms a dimer,<sup>14</sup> which might not be degraded as rapidly as the normal TIMP-3, and may accumulate in Bruch's membrane. Because the mutant TIMP-3 appears to be able to inhibit the activity of MMPs<sup>14</sup> it might lead to an exaggerated inhibition of protease activity, which, in turn, to an increased accumulation of extracellular material. As the mutant TIMP-3 is only one amino acid different from the normal TIMP-3, it is believed that the antibody against TIMP-3 was immunopositive for both the mutant and the normal protein. Although immunohistochemistry is not a quantitative method for the assessment of the amount of protein present, our findings of increased extent of TIMP-3 immunoreactivity supports the notion that mutant TIMP-3 may accumulate. There is also an interesting parallel in that there is more TIMP-3 protein in eyes of AMD donors than in those of age-matched control subjects.<sup>15</sup>

## TIMP-3 Mutation and Elastin

The localization of TIMP-3 and elastin was similar. They were both present in the elastic layer of Bruch's membrane, in the elastic layer of choroidal vessels, and in the basement membrane of the nonpigmented ciliary epithelium (zonules contain immature elastic fibers). This suggests that TIMP-3 might play a role in the turnover of elastic fibers. Although mutant TIMP-3 might inhibit protease activity, it is not certain whether its actions are entirely normal. It is possible that mutant TIMP-3 in some way fails to protect elastic fibers, leading to the damage seen in SFD.

## TIMP-3 Mutation and Choroidal Neovascularization

There is a potential paradox in that TIMP-3 has been reported to have an inhibitory effect on angiogenesis,<sup>16</sup> and yet in 2 of the 10 symptomatic patients with SFD in a family survey has central visual loss due to choroidal neovascularization.<sup>3</sup> Mutant TIMP-3 may not exhibit antiangiogenic properties. Alternatively, the breaks in the Bruch's membrane might be too extensive to contain the extension of

new vessels despite extensive TIMP-3 accumulation in Bruch's membrane.

## SUMMARY

TIMP-3 is present in Bruch's membrane and the basement membrane of the nonpigmented ciliary epithelium. Although direct evidence is awaited, it is possible to speculate that the genetic mutation in *TIMP-3* might have led to the deposits in both of these locations secondary to the accumulation of the active mutant TIMP-3. In SFD, altered elastic fibers in the Bruch's membrane might be expected to lead to choroidal neovascularization, which dominates the clinical picture. SFD originally was named because of its clinical features. In view of the ciliary body pathology described here, the condition might be better termed Sorsby's ocular epitheliopathy.

## References

1. Sorsby A, Mason MEJ, Gardener N. A fundus dystrophy with unusual features. *Br J Ophthalmol*. 1949;33:67-97.
2. Hamilton WK, Ewing CC, Ives EJ, Carruthers JD. Sorsby's fundus dystrophy. *Ophthalmology*. 1989;96:1755-1762.
3. Polkinghorne PJ, Capon MR, Berninger T, Lyness AL, Sehmi K, Bird AC. Sorsby's fundus dystrophy. A clinical study. *Ophthalmology*. 1989;96:1763-1768.
4. Capon MR, Polkinghorne PJ, Fitzke FW, Bird AC. Sorsby's pseudo-inflammatory macula dystrophy—Sorsby's fundus dystrophies. *Eye*. 1988;2:114-122.
5. Weber BH, Vogt G, Wolz W, Ives EJ, Ewing CC. Sorsby's fundus dystrophy is genetically linked to chromosome 22q13-qter. *Nat Genet*. 1994;7:158-161.
6. Weber BH, Vogt G, Pruett RC, Stohr H, Felbor U. Mutations in the tissue inhibitor of metalloproteinases-3 (TIMP3) in patients with Sorsby's fundus dystrophy. *Nat Genet*. 1994;8:352-356.
7. Fariss RN, Apte SS, Olsen BR, Iwata K, Milam AH. Tissue inhibitor of metalloproteinases-3 is a component of Bruch membrane of the eye. *Am J Pathol*. 1997;150:323-328.
8. Della NG, Campochiaro PA, Zack DJ. Localization of TIMP-3 mRNA expression to the retinal pigment epithelium. *Invest Ophthalmol Vis Sci*. 1996;37:1921-1924.
9. Ashton N, Sorsby A. Fundus dystrophy with unusual features: a histological study. *Br J Ophthalmol*. 1951;35:751-764.
10. Capon MR, Marshall J, Krafft JI, Alexander RA, Hiscott PS, Bird AC. Sorsby's fundus dystrophy. A light and electron microscopic study. *Ophthalmology*. 1989;96:1769-1777.
11. Kuntz CA, Jacobson SG, Cideciyan AV, et al. Sub-retinal pigment epithelial deposits in a dominant late-onset retinal degeneration. *Invest Ophthalmol Vis Sci*. 1996;37:1772-1782.
12. Duvall J, McKechnie NM, Lee WR, Rothery S, Marshall J. Extensive subretinal pigment epithelial deposit in two brothers suffering from dominant retinitis pigmentosa. A histopathological study. *Graefes Arch Clin Exp Ophthalmol*. 1986;24:299-309.
13. Brosnahan DM, Kennedy SM, Converse CA, Lee WR, Hammer HM. Pathology of hereditary retinal degeneration associated with hypobetalipoproteinemia. *Ophthalmology*. 1994;101:38-45.
14. Langton KP, Barker MD, McKie N. Localization of the functional domains of human tissue inhibitor of metalloproteinases-3 and the effects of a Sorsby's fundus dystrophy mutation. *J Biol Chem*. 1998;273:16778-16781.
15. Kamei M, Hollyfield JG. TIMP-3 in Bruch's membrane: changes during aging and in age-related macular degeneration. *Invest Ophthalmol Vis Sci*. 1999;40:2367-2375.
16. Anand-Apte B, Pepper MS, Voest E, et al. Inhibition of angiogenesis by tissue inhibitor of metalloproteinase-3. *Invest Ophthalmol Vis Sci*. 1997;38:817-823.